

Enhancing PV Efficiency using Direct Cooling with CuO Nanofluid

Nikhil K. Purwant^{1*}, and Avinash M. Badadhe²

¹Savitribai Phule Pune University, JSPM Rajarshi Shahu College of Engineering, Department of Mechanical Engineering, Tathawade, Pimpri-Chinchwad, Pune, Maharashtra, India

²Savitribai Phule Pune University, JSPM Rajarshi Shahu College of Engineering, Department of Automation & Robotics, Tathawade, Pimpri-Chinchwad, Pune, Maharashtra, India

purwantn@gmail.com, avi_badadhe@rediffmail.com

Abstract

This study experimentally evaluates the use of copper oxide (CuO)-water nanofluids as a direct cooling medium for photovoltaic (PV) panels to improve their thermal management and electrical performance. Experiments were conducted over nanoparticle concentrations of 1-5% and flow rates ranging from 0.07 to 0.11 kg/s. Key performance indicators, including panel surface temperature, electrical efficiency, power output, and coolant evaporation, were measured. Compared to conventional water cooling, the CuO nanofluid reduced panel temperature by up to 9.25°C, increased electrical efficiency from 16.32% to 17.60%, enhanced maximum power output from 47.98 W to 51.75 W, and decreased evaporative losses from 34.14% to 30.77%. Uncertainty analysis conducted using the Mean Absolute Percentage Error (MAPE) method showed uncertainties of $\pm 0.718\%$ for electrical efficiency, confirming the reliability of the results. The findings demonstrate the significant potential of CuO nanofluids in direct PV cooling, promising improved energy yield and durability in hot climates. Practical considerations regarding nanofluid stability, viscosity, and system scalability are discussed to support future commercial applications.

Index-words: CuO nanofluid cooling, Photovoltaic (PV) panels, Thermal management, Electrical efficiency, Evaporation suppression, Renewable energy.

I. Introduction

The depletion of non-renewable energy resources has accelerated the adoption of renewable alternatives such as solar energy, which offers approximately 5000 trillion kWh annually in India [1]. Photovoltaic (PV) panels convert solar radiation into electricity through semiconductor devices [2]. However, prolonged solar exposure increases PV cell temperatures, leading to an efficiency drop of nearly 0.45% for every 1 °C rise [3]. Therefore, efficient thermal management strategies are essential to sustain PV performance. In this context, thermal management refers to methods designed to regulate the temperature of PV panels by removing excess heat, thereby preserving electrical efficiency.

Numerous cooling techniques have been proposed. Ridha Hasan et al. (2022) developed a CFD model validated by experiments, showing that front-face water cooling achieved a 50.2% reduction in surface temperature and a 22.83% increase in efficiency [4]. Further, Bouafia and Abdallah (2024) showed through

numerical modeling that combined PV/T cooling with water reduces PV temperature by up to 22°C, resulting in an approximate 3.1% boost in electrical efficiency [5]. Dorobanțu et al. (2013) demonstrated that water cooling reduced PV temperature by 4 °C and improved efficiency by 12% [6]. Moharram et al. (2013) designed an automated cooling system that activated above 45 °C, lowering panel temperature by 10 °C at 2 °C/min [7]. Abdul Gafar et al. (2014) tested partial submersion, showing an 11% efficiency gain at 6 cm immersion depth [8]. Sornek et al. (2023) reported that direct water cooling (DWC) improved output by 3.0–12.0% in the lab and 1.2–13.7% under real conditions, with thermal recovery up to 420.6 W and economic feasibility demonstrated through a 7.6–9.1 year payback [9]. Similarly, Mah et al. (2019) applied water-film cooling on rooftop arrays, achieving a 15% output increase and sustainable operation via rainwater harvesting [10].

Other strategies include rear-side spray cooling, which improved electrical output by 7.8% and reduced temperature by 28.2% [11], and high-flow

spray cooling, which yielded 16.65% efficiency improvement [12]. Hadipour et al. (2020) reported a 33.3% efficiency increase using spray cooling [13], while Nizetic et al. (2015) observed a 14.1% improvement [14]. A comparative review by Raad et al. (2025) highlighted that spray cooling and V-shaped aluminum channels improved efficiency by 7.8% and 4.4%, respectively, whereas evaporative cooling pads and integrated PV/thermal systems with earth-to-water heat exchangers achieved 4.7–12% and 1.02–1.41% gains [15]. Collectively, studies confirm that direct water-contact methods, such as immersion, spray, and jet impingement, deliver high heat transfer rates and significant efficiency gains.

Beyond water-based methods, nanofluids have attracted attention for their superior thermal conductivity. Lee et al. (1999) demonstrated that CuO/ethylene glycol nanofluids improved conductivity by >20% at 4% concentration, outperforming Al₂O₃-based nanofluids. Similarly, CuO-based nanofluids consistently exceeded the thermal performance of Al₂O₃ across different base fluids [16]. Despite such promising results, limited studies have experimentally applied CuO–water nanofluids directly for PV cooling, leaving a gap in experimental validation for real-world conditions.

Recent investigations have further expanded the frontiers of photovoltaic cooling technology through integrated nano-enhanced fluids and hybrid thermal management approaches. Azeez et al. (2025) conducted an extensive economic and environmental feasibility analysis of photovoltaic thermal systems combining passive cooling, nanofluids, and phase change materials, demonstrating potential for optimized heat dissipation and improved lifecycle sustainability [17]. In parallel, Prakash et al. (2024) explored advanced nanofluid formulations tailored for PV cooling applications, emphasizing the critical balance between enhanced thermal conductivity and practical challenges such as fluid stability and increased viscosity at higher nanoparticle concentrations [18]. These key studies complement the current investigation by providing a broader context of state-of-the-art cooling enhancements, highlighting that CuO nanofluid-based direct cooling methods continue to be strong candidates for efficient thermal regulation when combined with optimized fluid properties and system parameters.

Beyond technical performance, PV cooling technologies have direct relevance to the United Nations Sustainable Development Goals (SDGs). By

increasing the energy yield of PV panels, such methods contribute to SDG 7 (Affordable and Clean Energy) and SDG 13 (Climate Action), which emphasize clean energy access and emissions reduction [19]. Nerini et al. (2018) highlight that energy technologies offering efficiency improvements create strong synergies with multiple SDGs [20], while recent work in the Alexandria Engineering Journal has stressed that advanced PV cooling strategies are critical enablers for sustainable renewable energy systems [21].

This research addresses that gap by experimentally investigating the performance of a PV system cooled directly with CuO–water nanofluid, compared against conventional water cooling. The study explores varying nanoparticle concentrations and mass flow rates to assess their effects on surface temperature, efficiency, power output, and evaporative losses. By benchmarking against water-based cooling, this work contributes novel evidence of the practicality and superiority of CuO nanofluids for direct PV cooling, offering new insights into sustainable thermal management solutions.

II. Nanofluid preparation

For the experimental synthesis of copper oxide (CuO) nanoparticles, analytical reagent-grade copper(II) chloride (CuCl₂) and potassium hydroxide (KOH) pellets, both procured from Merck India Ltd., were utilized. The preparation method followed a modified protocol based on the technique reported by Tran and Nguyen (2014) [22]. A 0.1 M aqueous solution of copper(II) chloride and a 0.5 M KOH solution were prepared separately using deionized water. Under atmospheric pressure and constant magnetic stirring, the KOH solution was gradually introduced dropwise into the copper chloride solution to ensure homogeneous mixing. The resulting mixture was then heated at 70 °C for 60 minutes, leading to the formation of a dark black precipitate of copper hydroxide. This precipitate was filtered repeatedly using Whatman filter paper until a solid mass was obtained. The solid was subsequently annealed at 200 °C in an electric muffle furnace for three hours to induce crystallization. After cooling, the material was finely ground into powder form for further analysis. These nanoparticles were then submitted to Savitribai Phule Pune University for characterization, and the resulting data were collected. The preparation method of the CuO nanoparticles is illustrated in Figure 1a, while the stability of the prepared nanofluid was evaluated using a magnetic stirrer, as depicted in Figure 1b.

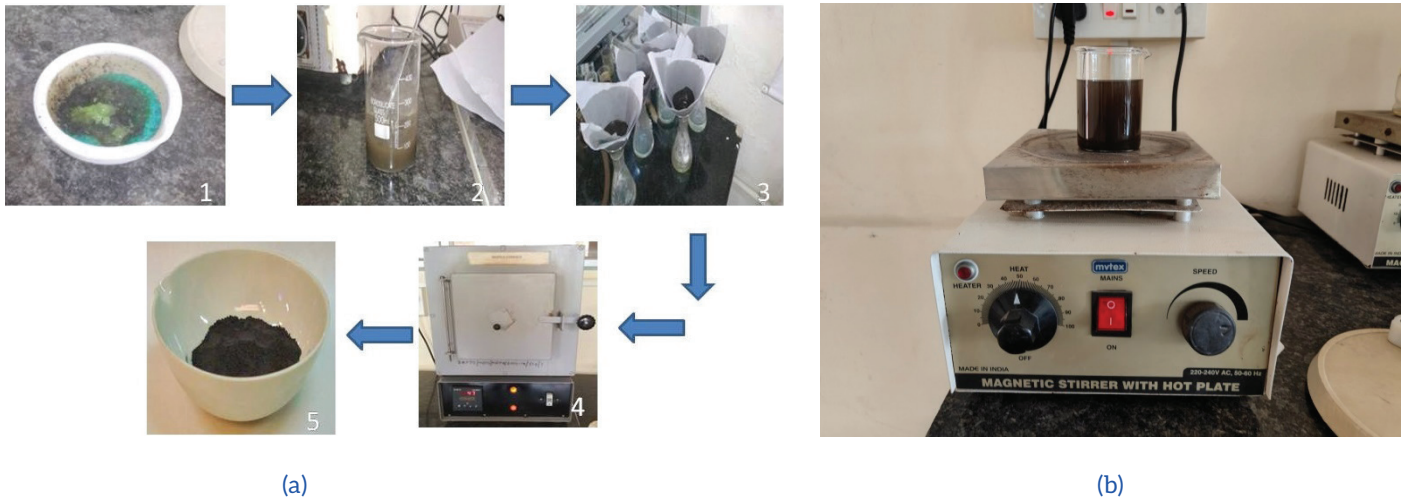


Figure 1: (a) Methodology for CuO nanoparticle preparation, (b) Magnetic stirrer with hot plate.

SEM micrographs revealed that the synthesized CuO nanoparticles exhibited flake-like structures with irregular geometries and grain boundaries.

From the micrograph of copper oxide, figure 2, one can observe spherical-shaped nanoparticles. The average nanoparticle size achieved is 77.54nm.

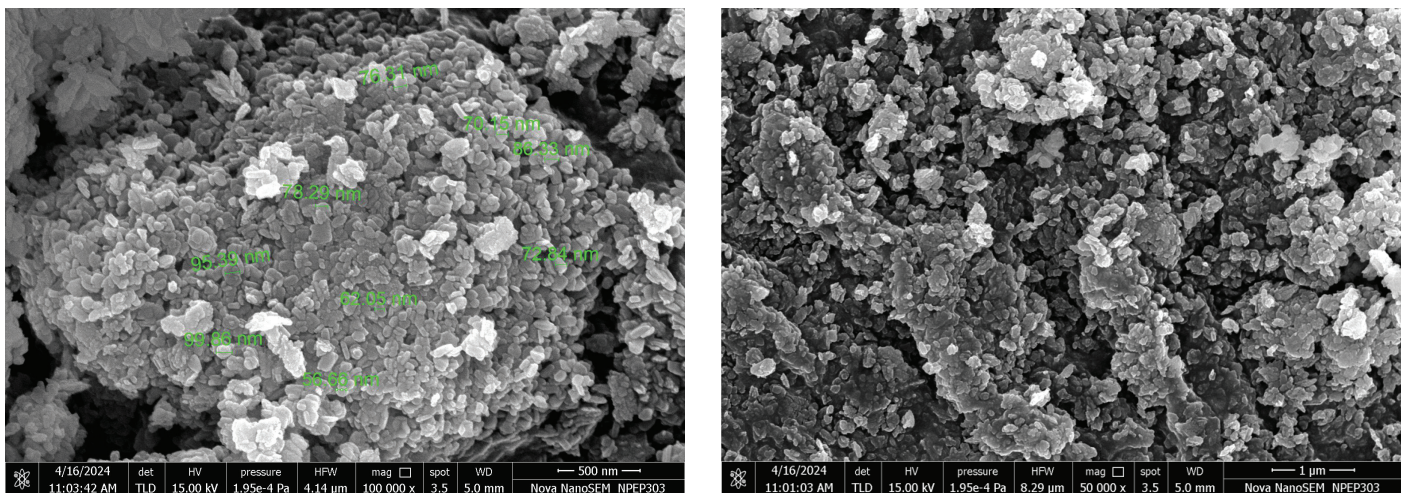


Figure 2: Micrographs of CuO.

A. Characterization of Nanofluid

The thermo-physical characteristics of CuO-Water nanofluid were calculated using an expression available in the literature [23] and tabulated in Table 1.

- Density:**

$$\rho_{nfs} = \rho_{ps} \phi + \rho_{bfs} (1 - \phi) \tag{1}$$

Where, ρ_{nfs} is the density of nanofluids; ρ_{ps} is the density of nanoparticles; ρ_{bfs} is the density of base fluid; and ϕ is the volume concentration

- Specific heat:**

$$C_{pnfs} = \phi C_{ps} (1 - \phi) C_{pbfs} \tag{2}$$

The equation was further modified for dilute concentration of nanofluid by Buongiorno (2005) [24] and expressed as

$$C_{pnfs} = \frac{\phi C_{ps} \rho_s + (1 - \phi) C_{pbfs} \rho_{bfs}}{\rho_{nfs}} \tag{3}$$

Where, C_{pnfs} is the specific heat of the nanofluid, C_{ps} is the specific heat of the nanoparticles, and C_{pbfs} is the specific heat of the base fluid.

• **Thermal conductivity:**

Hamilton and Crosser (1962) [25] gave the relation for the effective thermal conductivity (k) of nanofluids as follows

$$\frac{k_{nfs}}{k_{bfs}} = \frac{\frac{k_p}{k_{bfs}} + (n - 1) - (n - 1)(1 - \frac{k_p}{k_{bfs}})\phi}{\frac{k_p}{k_{bfs}} + (n - 1) + (1 - \frac{k_p}{k_{bfs}})\phi} \quad (4)$$

Where n is an empirical factor for shape; k_{nfs} is the thermal conductivity of the nanofluid; k_{bfs} is the thermal conductivity of the nanofluid base fluid

Table 1: Nanofluid properties

	Density, ρ (kg/m ³)	Specific Heat, Cp (J/kg-K)	Thermal conductivity, k (W/m-k)
Water + 1% CuO Np	1051.03	3957.8	0.6178
Water + 2% CuO Np	1105.06	3757.33	0.6359

Water + 3% CuO Np	1159.09	3575.55	0.6543
Water + 4% CuO Np	1213.12	3409.97	0.6732
Water + 5% CuO Np	1267.15	3258.5	0.6924

B. Experimental setup and method

To construct a physical model, two 100 W-rated PV panels were utilized. The first panel served as the baseline, operating with a conventional water-cooling system. The second panel was enhanced by incorporating a CuO-water nanofluid cooling system. The cooling setup included essential components such as a water pump, flow meter, control valve, distributing pipes, and a storage tank, as illustrated in Figure 3. To ensure even distribution of cooling water across the front face of the panel, a distributing pipe with 50 nozzles, each 0.5 cm in diameter, was used. All instruments employed in the experimental procedures were calibrated against reference standards to ensure consistent and repeatable measurements.

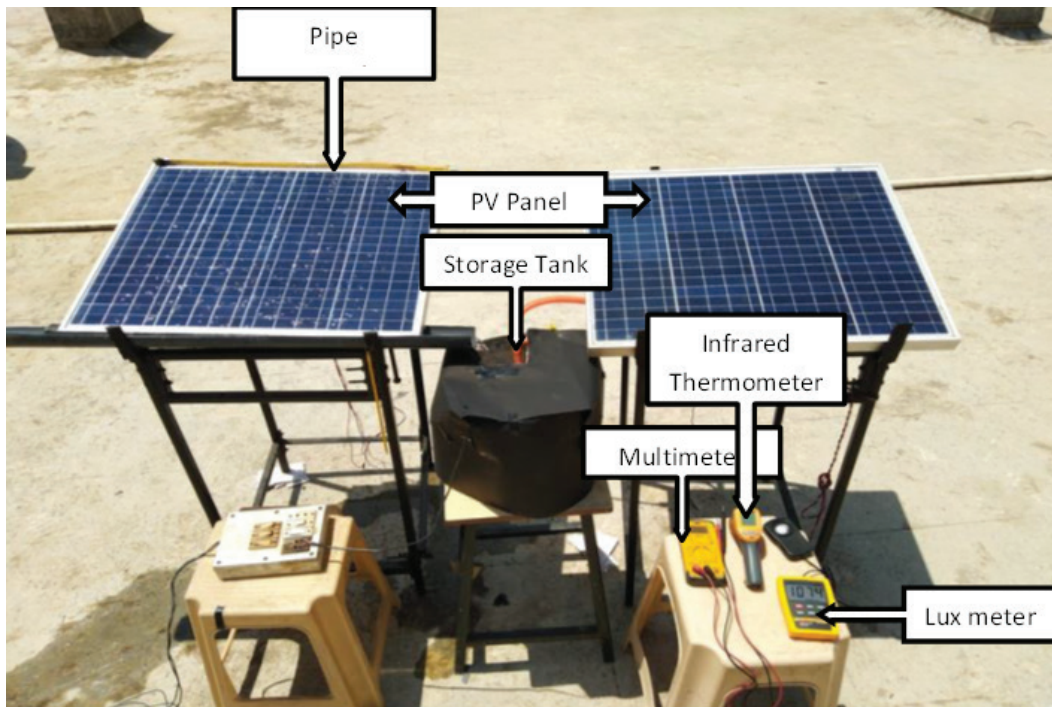


Figure 3: Experimental setup.

Field experiments were carried out at 18.7611° N latitude and 73.5572° E longitude, with the panels inclined at a 20° tilt. Based on the findings of Mani and Chako (1973) for India, the highest solar radiation occurs in April or May [26]; therefore, the experimental activities were scheduled in April. To maximize solar exposure, the tests were

performed on clear-sky days. During the course of experimentation, wind speeds ranged between 1.0 m/s and 1.5 m/s. Measurements were recorded every 30 minutes from 10:00 a.m. to 15:00 p.m., and the acquired data were utilized to determine and analyze the performance parameters. The electrical efficiency is expressed as,

$$\eta_{el} = \frac{P_{max}}{I_g \times A_c} \tag{5}$$

$$P_{max} = V \times I \tag{6}$$

Where P_{max} is the Maximum output power, voltage (V), and current (I) at the maximum power point, I_g is the incident solar radiation, and A_c is the PV area.

1. Uncertainty analysis

In experimental setups, every measured value is inherently associated with some degree of uncertainty, stemming from limitations such as the instrument’s minimum readable division and calibration accuracy, which must be carefully taken into account for reliable results. Measurements used to estimate cooling effectiveness, thermal gain, and electrical performance are subject to errors resulting from such inaccuracies. The uncertainty analysis for the experimental study was conducted using the Mean Absolute Percentage Error (MAPE) method, yielding uncertainties of $\pm 0.718\%$ in electrical efficiency.

Sukhatme proposed an impulse response and convolution-based approach to estimate transient model uncertainties in solar systems, demonstrating tank temperature variability within $\pm 2.2\text{ }^\circ\text{C}$ and reducing computational effort [27]. Facao et al. (2006) applied a linear regression uncertainty analysis to plate-type solar collectors, distinguishing between systematic and random error components for precise correlated uncertainty calculation [28]. The ANSI/ASME PTC 19.1-1985 standard for uncertainty evaluation in photovoltaic performance, summarized by Wells, provides comprehensive procedures to combine systematic and random errors for reliable measurement reporting [29].

In this study, the uncertainty quantification employs the Kline and McClintock propagation of error method, which frames uncertainties as intervals where the true values plausibly reside. This technique systematically incorporates uncertainties from all measured variables influencing electrical efficiency, yielding a rigorous overall uncertainty estimation for the experimental outcomes.

Table 2: Instruments with their individual uncertainty

Sr No.	Quantity	Instrument	Unit	accuracy
1	Mass Flow rate	Rotameter	Kg/sec	$\pm 1\%$
2	Electrical gain	Multimeter	A, V	$\pm 2\%$
3	Temperature	Infrared Thermometer	$^\circ\text{C}$	$\pm 1\%$
4	Solar radiation	Lux meter	W/m^2	$\pm 2\%$
5	Area	Measuring tape	M	$\pm 1\%$

The overall performance of the PVT collector can be expressed as a function of independent variables, including mass flow rate (m), temperature difference ($T_{out}-T_{in}$), collector area (A_c), solar radiation (I_g), open circuit voltage of the PV panel (V), and short circuit current (I). The measurement errors associated with these variables are represented as w_m , $w_{T_{out}}$, $w_{T_{in}}$, w_A , w_{I_g} , w_V , and w_I , respectively.

The total uncertainty of the collector’s performance can then be determined by applying the general formula provided by Kline and McClintock, which combines the individual measurement uncertainties through the root-sum-square of the partial derivatives of the performance function with respect to each variable, multiplied by their respective errors.

$$w_R = \pm \sqrt{\left(\frac{\partial R}{\partial x_1} w_1\right)^2 + \left(\frac{\partial R}{\partial x_2} w_2\right)^2 + \dots + \left(\frac{\partial R}{\partial x_n} w_n\right)^2} \tag{7}$$

Where $R \{m, T_{out}, T_{in}, A_c, I_g, V, I\}$ are the average values of parameters

Hence, by utilizing the appropriate equation, the uncertainty in electrical performance can be determined as follows,

$$w_{\eta_E} = \pm \sqrt{\left(\frac{\partial \eta_E}{\partial P} w_P\right)^2 + \left(\frac{\partial \eta_E}{\partial V} w_V\right)^2 + \left(\frac{\partial \eta_E}{\partial A_c} w_{A_c}\right)^2 + \left(\frac{\partial \eta_E}{\partial I_g} w_{I_g}\right)^2} \tag{8}$$

The relative uncertainty is assessed to determine the accuracy of the observations and is expressed using the following equation.

$$U_a = \pm \frac{\delta d}{d} \tag{9}$$

Where δd is the error value and d is the average value obtained during calculation.

III. Result and discussion

A. Analysis for PV Panel Surface Temperature

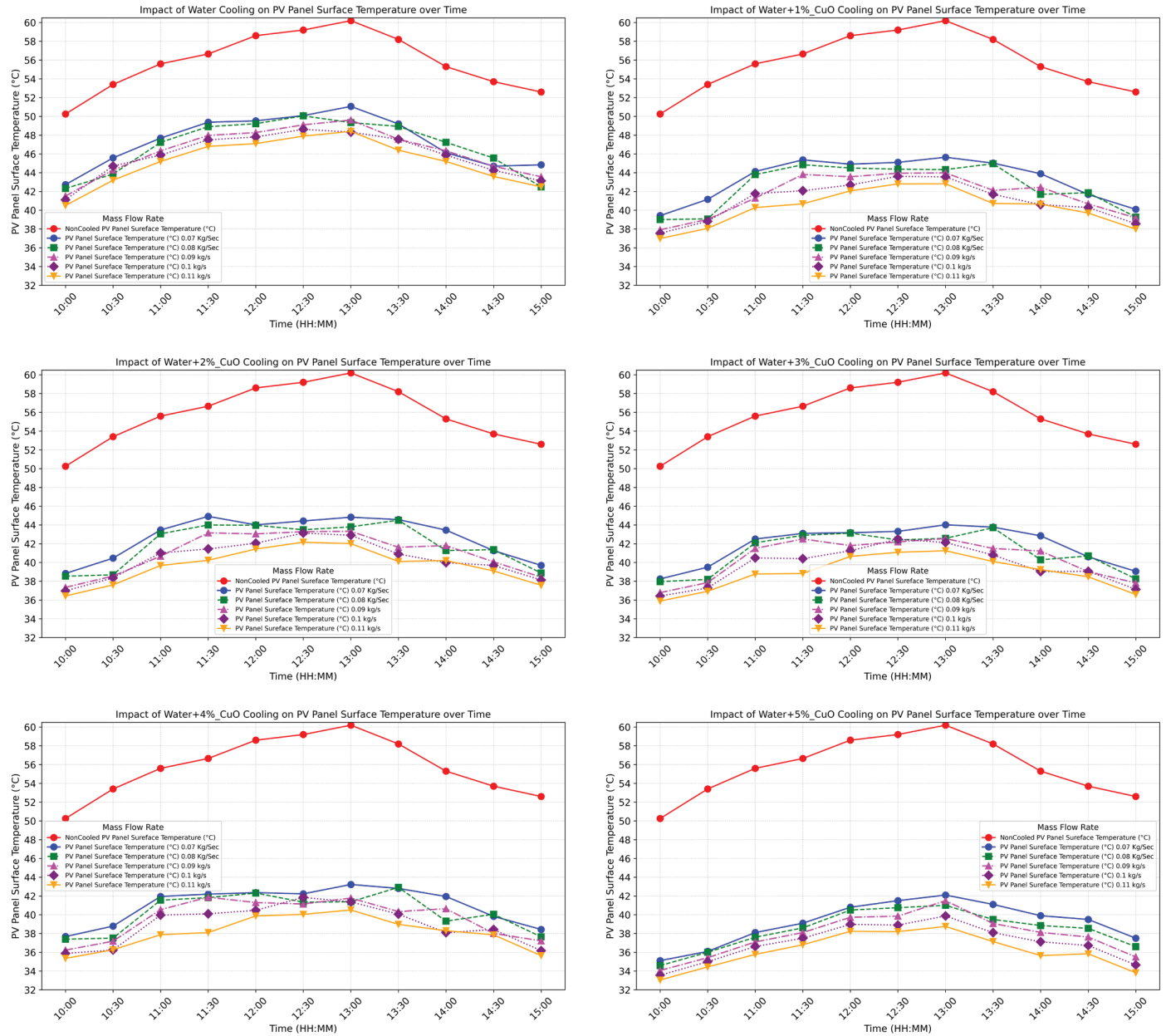


Figure 4: Impact of water and Water with different concentration of CuO Nanofluid Cooling on PV Panel Surface Temperature over time.

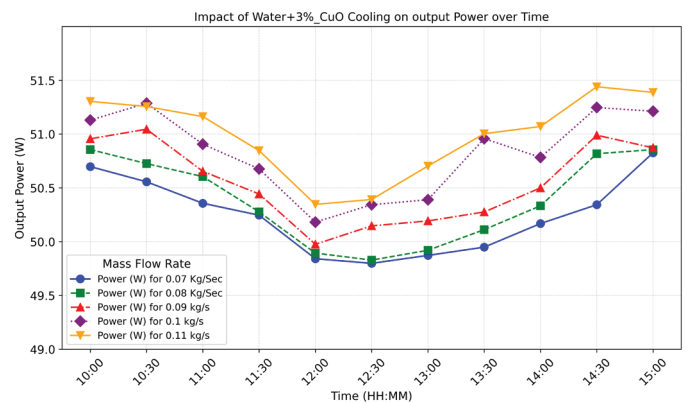
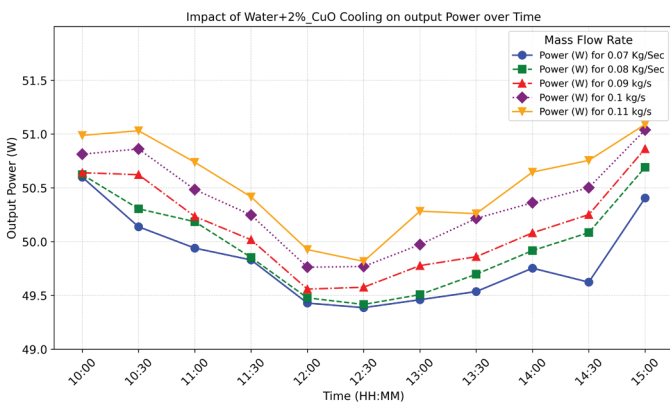
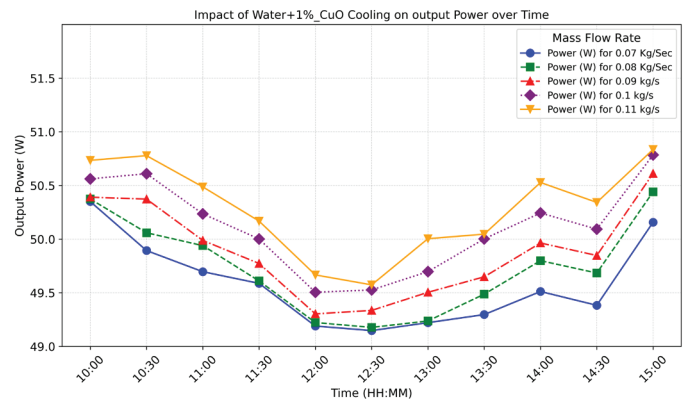
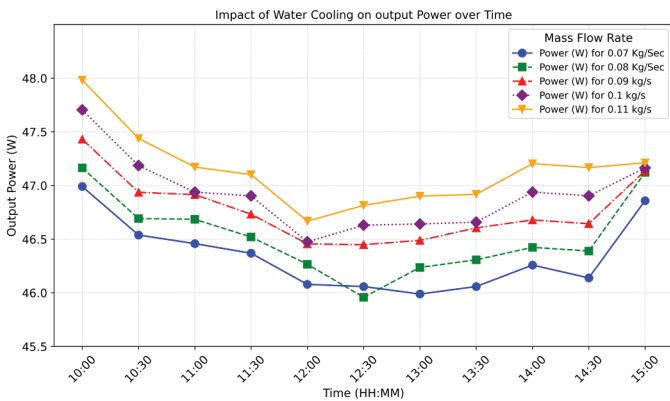
Table 3: Summary of PV panel surface temperature

Flow Rate (Kg/s)	Water	Water+1% CuO	Water+2% CuO	Water+3% CuO	Water+4% CuO	Water+5% CuO
0.07	51.06	45.65	44.91	44.24	43.58	42.10
0.08	50.06	44.96	44.51	43.71	42.92	41.34
0.09	49.61	43.98	43.32	42.54	41.87	41.50
0.1	48.62	43.61	43.14	42.49	41.85	39.87
0.11	48.40	42.82	42.16	41.25	40.51	39.15

A detailed comparative study was conducted to evaluate the effect of CuO-water nanofluids at varying concentrations (1% to 5%) and flow rates (0.07 to 0.11 kg/s) on PV panel surface temperature reduction, as shown in Figure 4. Table 3 indicates that, at a mass flow rate of 0.07 kg/s, the PV panel surface temperature with water cooling was 51.06 °C. The use of CuO nanofluids at concentrations of 1%, 2%, 3%, 4%, and 5% resulted in respective surface temperatures of 45.65 °C, 44.91 °C, 44.24 °C, 43.58 °C, and 42.10 °C. This trend indicates that increasing nanoparticle concentration enhances heat dissipation. At 0.08 kg/s, water cooling produced a surface temperature of 50.06 °C, whereas the 1% to 5% CuO nanofluids yielded 44.96 °C, 44.51 °C, 43.71 °C, 42.92 °C, and 41.34 °C, respectively. A clear temperature drop was observed with higher nanofluid concentration. The 0.09 kg/s flow rate followed a similar pattern, with water at 49.61 °C, and CuO nanofluids achieving 43.98 °C (1%), 43.32 °C

(2%), 42.54 °C (3%), 41.87 °C (4%), and 41.50 °C (5%). At 0.10 kg/s, water cooling resulted in 48.62 °C, while CuO-based cooling reduced the temperature further to 43.61 °C (1%), 43.14 °C (2%), 42.49 °C (3%), 41.85 °C (4%), and 39.87 °C (5%). Finally, at the highest tested flow rate of 0.11 kg/s, the lowest surface temperature was achieved with 5% CuO nanofluid at 39.15 °C, compared to 48.40 °C with water. Other nanofluid temperatures at this flow rate were 42.82 °C (1%), 42.16 °C (2%), 41.25 °C (3%), and 40.51 °C (4%). This comprehensive data clearly demonstrates that both increasing nanoparticle concentration and flow rate significantly enhance PV panel cooling. The 5% CuO nanofluid at 0.11 kg/s offers optimal performance with a maximum temperature reduction of 9.25 °C compared to water cooling alone.

B. Result analysis for Output Power



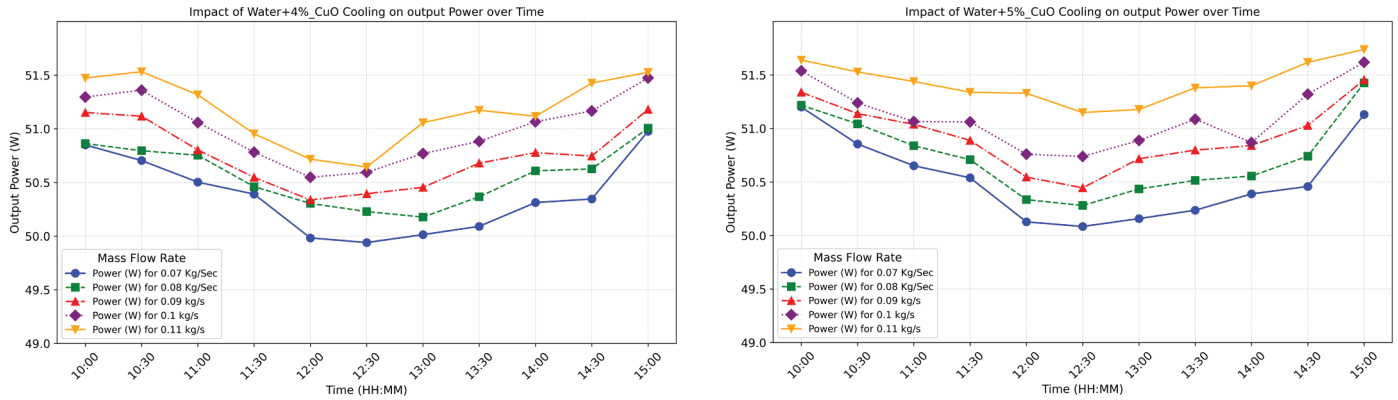


Figure 5: Impact of water and Water with different concentration of CuO Nanofluid Cooling on PV Panel Output power over time.

Table 4: Summary of maximum output power

Flow Rate (Kg/s)	Water	Water+1% CuO	Water+2% CuO	Water+3% CuO	Water+4% CuO	Water+5% CuO
0.07	46.99	50.35	50.60	50.83	50.98	51.20
0.08	47.16	50.44	50.69	50.86	51.01	51.42
0.09	47.43	50.61	50.86	51.05	51.18	51.45
0.1	47.70	50.78	51.04	51.29	51.47	51.62
0.11	47.98	50.84	51.09	51.44	51.53	51.74

Figure 5 shows the enhancement in maximum power output of PV modules through front-face cooling using CuO-water nanofluid, which was experimentally analyzed under five different flow rates and nanoparticle concentrations. Water was used as the reference coolant for comparative analysis. Table 4 indicates that, at a mass flow rate of 0.07 kg/s, the PV panel with water cooling delivered a power output of 46.99 W. With 1% CuO nanofluid, the output improved to 50.35 W, increasing further to 50.60 W at 2%, 50.83 W at 3%, 50.98 W at 4%, and peaking at 51.20 W with 5% CuO. This reflects a 9.1% enhancement compared to water at the same flow rate, attributed to superior heat extraction capacity. As the flow rate increased to 0.08 kg/s, water cooling yielded 47.16 W. CuO nanofluids resulted in 50.44 W (1%), 50.69 W (2%), 50.86 W (3%), 51.01 W (4%), and 51.42 W (5%). Notably, a similar increasing trend was observed, though the incremental gains reduced slightly due to approaching saturation. At 0.09 kg/s, the recorded output using water

was 47.43 W, whereas the CuO nanofluid system yielded 50.61 W (1%), 50.86 W (2%), 51.05 W (3%), 51.18 W (4%), and 51.45 W (5%). The enhancements ranged approximately from 3.3% to 6.8%, suggesting continued performance improvement with higher particle loading. Further increasing to 0.10 kg/s, the PV panel with water cooling produced 47.70 W. With CuO nanofluids, outputs were 50.78 W (1%), 51.04 W (2%), 51.29 W (3%), 51.47 W (4%), and 51.62 W (5%). Here, the difference between 1% and 5% corresponds to about a 1.6 W gain and a 3.2% improvement, at the maximum flow rate of 0.11 kg/s, water cooling produced 47.98 W, while CuO nanofluid outputs were 50.84 W (1%), 51.09 W (2%), 51.44 W (3%), 51.53 W (4%), and 51.74 W (5%). While the performance gain remained evident, marginal improvements diminished beyond 4%, indicating a plateau. Overall, the 5% CuO nanofluid provided consistent enhancement across all flow rates, with improvements over water ranging from approximately 7.4% to 8%.

C. Result analysis for Electrical Efficiency

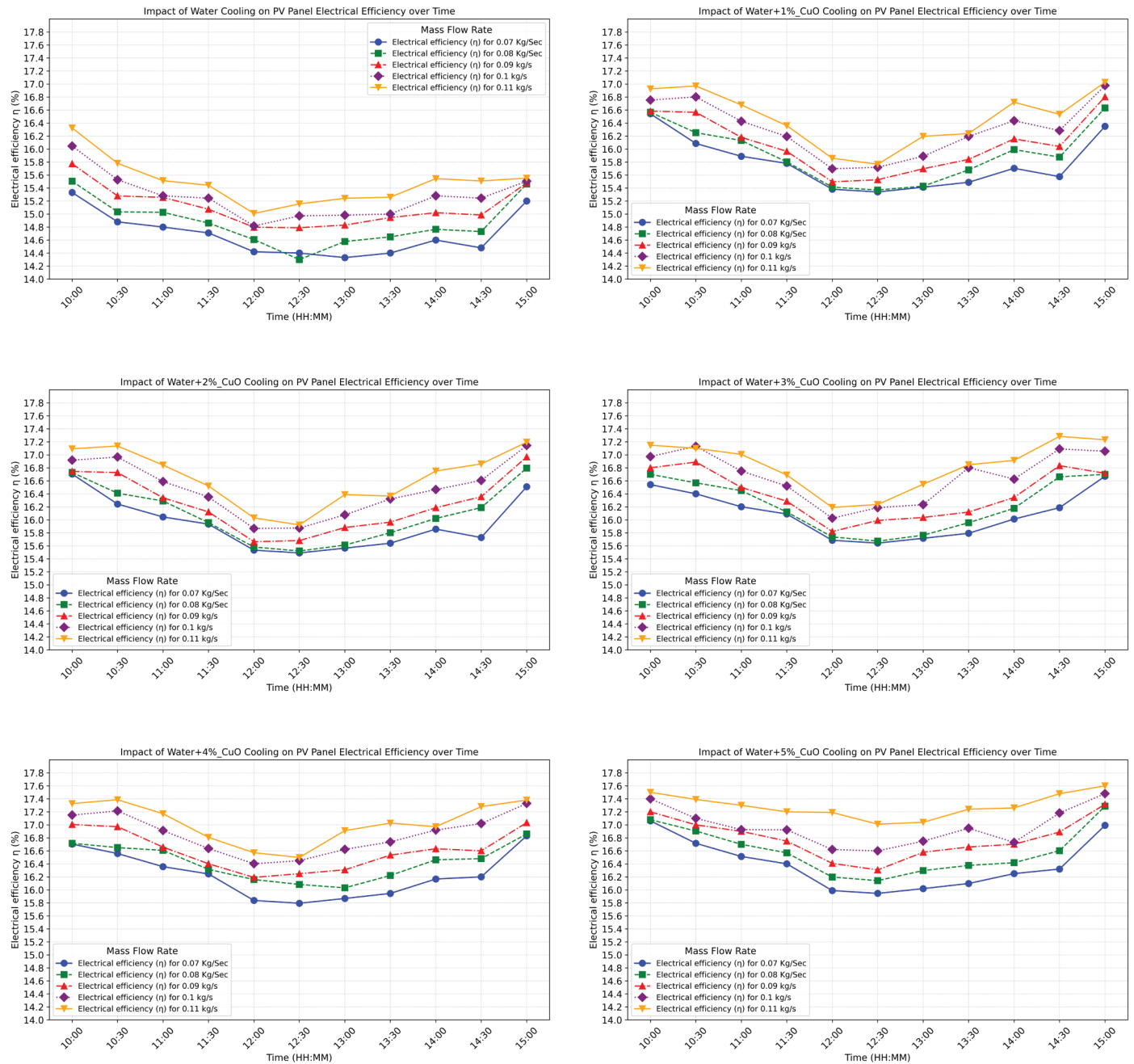


Figure 6: Impact of water and Water with different concentration of CuO Nanofluid Cooling on PV Panel Efficiency over time.

Table 5: Summary of maximum electrical efficiency

Flow Rate (Kg/s)	Water	Water+1% CuO	Water+2% CuO	Water+3% CuO	Water+4% CuO	Water+5% CuO
0.07	15.33	16.54	16.70	16.67	16.83	17.06
0.08	15.51	16.63	16.80	16.70	16.86	17.29
0.09	15.77	16.80	16.97	16.89	17.03	17.32
0.1	16.05	16.98	17.14	17.13	17.33	17.48
0.11	16.32	17.03	17.19	17.28	17.39	17.60

The experimental investigation assessed the electrical efficiency enhancement of photovoltaic (PV) panels utilizing CuO–water nanofluids at varying volume concentrations (1%–5%) and flow rates (0.07–0.11 kg/s), benchmarked against conventional water-cooled systems as per Figure 6. Table 5 highlights a consistent and measurable improvement in electrical performance with the incorporation of CuO nanoparticles, attributed to superior thermal regulation and reduced cell operating temperatures. At a mass flow rate of 0.07 kg/s, the PV panel cooled with water attained a baseline electrical efficiency of 15.33%. The integration of CuO nanofluid yielded a marked increase, achieving 16.54% (1% CuO), 16.70% (2% CuO), 16.67% (3% CuO), 16.83% (4% CuO), and a peak value of 17.06% for the 5% CuO nanofluid. This demonstrates a progressive enhancement of 1.73 percentage points over water with increasing nanoparticle concentration, emphasizing the efficacy of higher particle loading for heat extraction. Increasing the flow rate to 0.08 kg/s, the electrical efficiency for water was observed at 15.51%. The CuO nanofluid system outperformed again, with efficiencies of 16.63% (1%), 16.80% (2%), 16.70% (3%), 16.86% (4%), and 17.29% (5%). The marginal gain from 4% to 5% indicates a saturation point where thermal advantage approaches an upper threshold. At a flow rate of 0.09 kg/s, the trend persisted with water yielding 15.77%, and CuO nanofluids achieving 16.80%, 16.97%, 16.89%, 17.03%, and 17.32% for 1% through 5% concentrations, respectively. This reflects that higher flow rates promote better heat transfer,

minimizing PV temperature rise and preserving electrical conversion efficiency. When the flow rate was increased to 0.10 kg/s, the water-cooled panel reported an efficiency of 16.05%, whereas CuO nanofluids produced 16.98%, 17.14%, 17.13%, 17.33%, and 17.48% for 1% to 5%, respectively. Notably, the 5% CuO nanofluid consistently delivered the peak performance, reiterating its superior heat absorption and dispersion capacity. At the highest tested flow rate of 0.11 kg/s, water cooling delivered 16.32% efficiency. CuO nanofluid results were 17.03%, 17.19%, 17.28%, 17.39%, and 17.60% corresponding to 1%–5% CuO concentrations. These outcomes reveal the diminishing incremental efficiency gains at higher nanoparticle concentrations, likely due to reaching thermophysical performance limits and potential increases in viscosity and flow resistance. In summary, across all tested flow rates and CuO concentrations, the incorporation of nanofluids led to a tangible improvement in electrical efficiency compared to water. The optimal condition for maximum electrical efficiency was identified as 5% CuO concentration at a 0.10 kg/s flow rate, achieving a peak efficiency of 17.60%, outperforming the water baseline by 1.73 percentage points. This confirms the strong potential of CuO-based nanofluids to enhance PV panel performance in thermal-management systems.

D. Coolant evaporation rate comparison

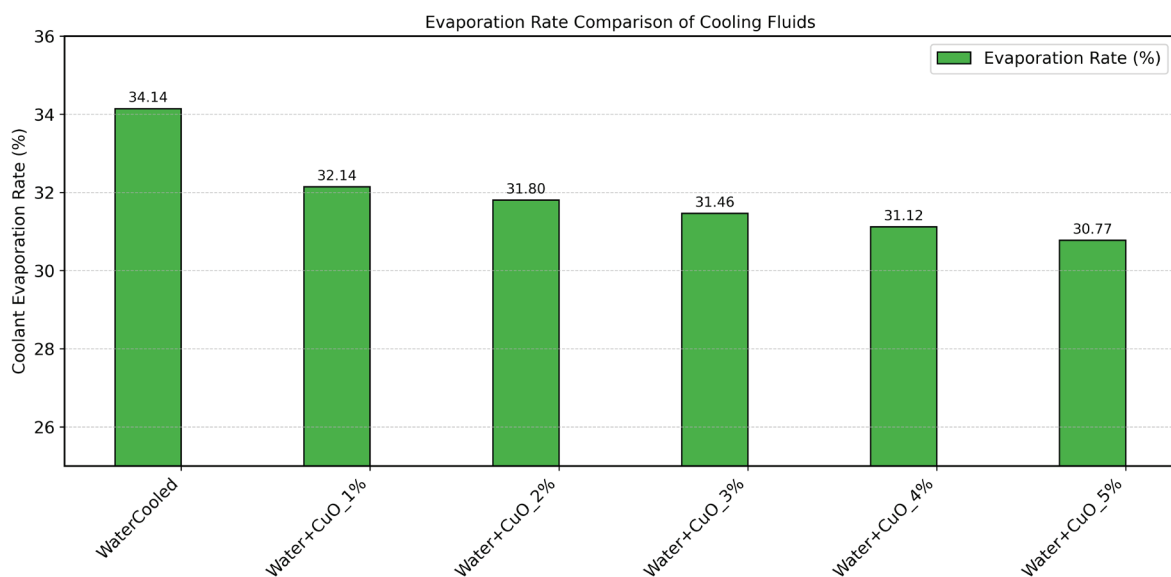


Figure 7: Evaporation rate of cooling fluid.

The reduction in evaporation rate of CuO–water nanofluids compared to pure water is primarily governed by their superior thermophysical and interfacial properties. The suspended CuO nanoparticles enhance the fluid's thermal conductivity, allowing rapid heat dissipation and minimizing localized overheating, which is a key trigger for evaporation in conventional water-based cooling [16], [24]. Nanoparticles also modify surface tension and vapor pressure characteristics at the liquid–air interface, where they can act as diffusion barriers that hinder vapor escape, thereby suppressing evaporation [18], [17]. Furthermore, the increased viscosity at higher nanoparticle concentrations dampens molecular mobility, adding another layer of resistance against evaporation [30].

This mechanism is consistent with the experimental evidence obtained in the present study. The water-cooled system exhibited the highest evaporation loss of 34.14%. With the incorporation of CuO nanoparticles, a gradual reduction was observed, with evaporation rates declining to 32.14% (1%), 31.80% (2%), 31.46% (3%), 31.12% (4%), and reaching the lowest value of 30.77% at 5% concentration, as shown in Figure 7. This steady trend demonstrates that the addition of nanoparticles not only improves thermal conductivity and heat capacity but also stabilizes the coolant by reducing evaporative losses. The improvement highlights that CuO nanofluids simultaneously address thermal regulation and durability, offering an advantage over pure water cooling in photovoltaic applications. Thus, CuO–water nanofluids exhibit dual benefits of enhanced heat transfer and lower evaporation, making them particularly suitable for sustained photovoltaic thermal cooling under prolonged solar irradiation [18], [17], [30].

E. Scalability and practical considerations of CuO Nanofluid Cooling in Large-Scale PV Systems

While the experimental validation in this study was conducted on 100 W lab-scale photovoltaic panels, translating these findings to large-scale PV installations entails distinctive thermal and hydraulic challenges. Large PV fields, characterized by significantly longer piping networks, elevated flow rates, and increased spatial exposure variations, can experience non-uniform cooling, pressure losses, and temperature gradients that reduce cooling system efficacy compared to controlled laboratory setups [31]. Hydraulic design optimization becomes

critical to ensure even coolant distribution and avoid channeling, while environmental factors such as wind disturbances further complicate the thermal management landscape [30], [32]. Additionally, upscaling nanofluid synthesis and managing supply chain logistics introduce considerable economic and operational complexities that must be systematically addressed through extended field trials and cost-benefit analyses.

Beyond scalability, practical aspects related to the use of high CuO nanoparticle concentrations (5%) warrant discussion. High nanoparticle loadings increase the viscosity of the cooling fluid, potentially resulting in higher pumping power demands that may offset thermal efficiency gains [17]. Furthermore, elevated concentrations increase the propensity for nanoparticle agglomeration and sedimentation, escalating the risk of clogging within distribution channels and impairing long-term reliability [18]. During the limited duration of our laboratory experiments, stability issues and clogging were not observed; however, these factors should be a primary focus in large-scale and long-duration implementations. Mitigation strategies such as nanoparticle surface functionalization, the use of dispersants, and routine maintenance procedures may alleviate these challenges and enhance the operational robustness of nanofluid cooling systems. Consequently, future research should emphasize extended stability tests, system optimization for pumping power efficiency, and field-scale validation to confirm the sustainable application of CuO nanofluids in photovoltaic thermal management.

IV. Conclusion

This investigation provides the first comprehensive experimental assessment of copper oxide (CuO)-water nanofluids for direct photovoltaic panel cooling across multiple nanoparticle concentrations (1-5%) and mass flow rates (0.07-0.11 kg/s). The experimental results demonstrate significant thermal management improvements when compared to conventional water-cooling systems.

The CuO nanofluid at 5% concentration achieved optimal performance, delivering a maximum surface temperature reduction of 9.25°C at 0.11 kg/s flow rate. Power output increased by 7-9% across all tested conditions, with electrical efficiency improvements ranging from 1.28 to 1.73 percentage points. The peak electrical efficiency of 17.60% was

recorded at 5% CuO concentration and 0.11 kg/s flow rate, representing a substantial enhancement over the water baseline of 16.32%. Additionally, coolant evaporation losses were reduced by over three percentage points, declining from 34.14% for water to 30.77% for the 5% CuO nanofluid.

The uncertainty analysis conducted using the Mean Absolute Percentage Error (MAPE) method confirmed measurement reliability with uncertainties of $\pm 0.718\%$ for electrical efficiency. These findings establish the superior thermophysical properties of CuO nanofluids, attributed to enhanced thermal conductivity, modified surface tension characteristics, and improved heat dissipation capabilities.

While laboratory-scale validation demonstrates clear performance advantages, practical implementation considerations must address potential challenges, including increased fluid viscosity, nanoparticle agglomeration risks, and pumping power requirements at higher

concentrations. Future research should focus on long-term stability assessment, field-scale validation, and comprehensive economic analysis to support commercial deployment.

The enhanced photovoltaic performance achieved through CuO nanofluid cooling technology contributes significantly to sustainable energy objectives, supporting United Nations Sustainable Development Goals 7 (Affordable and Clean Energy) and 13 (Climate Action). This approach offers particular value for large-scale solar installations in hot climates where conventional cooling methods may prove inadequate, ultimately advancing renewable energy efficiency and climate mitigation efforts.

Acknowledgements:

We extend our heartfelt thanks to the Savitribai Phule Pune University, Pune, Maharashtra, India, for their encouragement and support of our research work.

References

- [1] F. Ahmad and M. S. Alam, "Economic and ecological aspects for microgrids deployment in India," *Sustain Cities Soc*, vol. 37, pp. 407–419, Feb. 2018, doi: 10.1016/j.scs.2017.11.027.
- [2] U. of Michigan, "Solar PV Energy Factsheet," 2022. [Online]. Available: <https://css.umich.edu/publications/factsheets/energy/solar-pv-energy-factsheet>
- [3] E. Skoplaki and J. A. Palyvos, "On the temperature dependence of photovoltaic module electrical performance: A review of efficiency/power correlations," *Solar Energy*, vol. 83, no. 5, pp. 614–624, May 2009, doi: 10.1016/j.solener.2008.10.008.
- [4] M. R. Hasan, D. Mahdi, Ahmed, and Z. Abdulkareem, "PV panel Water Cooling Using Different Jet Nozzle Diameter," *Journal of Science and Engineering Applications*, vol. 4, 2022, [Online]. Available: <https://journals.iunajaf.edu.iq/index.php/JSEA/article/view/7>
- [5] S. Bouafia and M. Si Abdallah, "Numerical study of a solar PV/thermal collector under several conditions in Algeria," *Renewable Energy and Sustainable Development*, vol. 10, no. 2, p. 233, Sep. 2024, doi: 10.21622/resd.2024.10.2.900.
- [6] L. Dorobanțu, M. O. Popescu, C. L. Popescu, and A. Crăciunescu, "Experimental Assessment of PV Panels Front Water Cooling Strategy," *RE&PQJ*, vol. 11, no. 7, Jan. 2024, doi: 10.24084/repqj11.510.
- [7] K. A. Moharram, M. S. Abd-Elhady, H. A. Kandil, and H. El-Sherif, "Enhancing the performance of photovoltaic panels by water cooling," *Ain Shams Engineering Journal*, vol. 4, no. 4, pp. 869–877, Dec. 2013, doi: 10.1016/j.asej.2013.03.005.
- [8] S. A. Abdulgafar, O. S. Omar, and K. M. Yousif, "Improving The Efficiency Of Polycrystalline Solar Panel Via Water Immersion Method," *Int J Innov Res Sci Eng Technol*, vol. 3, no. 1, pp. 8127–8132, 2014.

- [9] K. Sornek, W. Goryl, and A. Głowacka, "Improving the performance of photovoltaic panels using a direct water cooling system," *Journal of Sustainable Development of Energy, Water and Environment Systems*, vol. 11, no. 4, pp. 1-24, Dec. 2023, doi: 10.13044/j.sdewes.d11.0468.
- [10] C.-Y. Mah, B.-H. Lim, C.-W. Wong, M.-H. Tan, K.-K. Chong, and A.-C. Lai, "Investigating the Performance Improvement of a Photovoltaic System in a Tropical Climate using Water Cooling Method," *Energy Procedia*, vol. 159, pp. 78-83, Feb. 2019, doi: 10.1016/j.egypro.2018.12.022.
- [11] P. Bevilacqua, R. Bruno, A. Rollo, and V. Ferraro, "A novel thermal model for PV panels with back surface spray cooling," *Energy*, vol. 255, p. 124401, Sep. 2022, doi: 10.1016/j.energy.2022.124401.
- [12] O. T. Laseinde and M. D. Ramere, "Efficiency Improvement in polycrystalline solar panel using thermal control water spraying cooling," *Procedia Comput Sci*, vol. 180, pp. 239-248, 2021, doi: 10.1016/j.procs.2021.01.161.
- [13] A. Hadipour, M. Rajabi Zargarabadi, and S. Rashidi, "An efficient pulsed- spray water cooling system for photovoltaic panels: Experimental study and cost analysis," *Renew Energy*, vol. 164, pp. 867-875, Feb. 2021, doi: 10.1016/j.renene.2020.09.021.
- [14] S. Nižetić, D. Čoko, A. Yadav, and F. Grubišić-Čabo, "Water spray cooling technique applied on a photovoltaic panel: The performance response," *Energy Convers Manag*, vol. 108, pp. 287-296, Jan. 2016, doi: 10.1016/j.enconman.2015.10.079.
- [15] H. Raad, S. Ali, J. Faraj, C. Castelain, K. Chahine, and M. Khaled, "Enhancing photovoltaic panel efficiency through Water-Cooling: A parametric comparative evaluation of energetic, economic, and environmental benefits," *Unconventional Resources*, vol. 7, p. 100208, Jul. 2025, doi: 10.1016/j.uncre.2025.100208.
- [16] S. Lee, S. U.-S. Choi, S. Li, and J. A. Eastman, "Measuring Thermal Conductivity of Fluids Containing Oxide Nanoparticles," *J Heat Transfer*, vol. 121, no. 2, pp. 280-289, May 1999, doi: 10.1115/1.2825978.
- [17] H. L. Azeez, A. Ibrahim, J. Kasprzak, B. O. Ahmed, A. H. A. Al-Waeli, and M. Jaber, "Economic and environmental feasibility analysis of a photovoltaic thermal system with passive cooling techniques, nanofluid, and phase changing materials," *Appl Therm Eng*, vol. 274, p. 126782, Sep. 2025, doi: 10.1016/j.applthermaleng.2025.126782.
- [18] A. Prakash, R. Kukreja, and P. Kumar, "Improving the performance of PV panel by using PCM with nanoparticles and Bifluid-A comprehensive review," *Materials Chemistry and Physics: Sustainability and Energy*, vol. 2, p. 100005, Mar. 2025, doi: 10.1016/j.mace.2024.100005.
- [19] N. United, "Transforming our world: The 2030 agenda for sustainable development," 2015. [Online]. Available: <https://sdgs.un.org/goals>.
- [20] F. Fusco Nerini *et al.*, "Mapping synergies and trade-offs between energy and the Sustainable Development Goals," *Nat Energy*, vol. 3, no. 1, pp. 10-15, Nov. 2017, doi: 10.1038/s41560-017-0036-5.
- [21] N. A. Moharram, A. H. Konsowa, A. I. Shehata, and W. M. El-Maghlany, "Sustainable seascapes: An in-depth analysis of multigeneration plants utilizing supercritical zero liquid discharge desalination and a combined cycle power plant," *Alexandria Engineering Journal*, vol. 118, pp. 523-542, Apr. 2025, doi: 10.1016/j.aej.2025.01.091.
- [22] T. H. Tran and V. T. Nguyen, "Copper Oxide Nanomaterials Prepared by Solution Methods, Some Properties, and Potential Applications: A Brief Review," *Int Sch Res Notices*, vol. 2014, pp. 1-14, Dec. 2014, doi: 10.1155/2014/856592.
- [23] R. Ramesh Kumar *et al.*, "Enhancing automotive cooling systems: composite fins and nanoparticles analysis in radiators," *Sci Rep*, vol. 14, no. 1, p. 3650, Feb. 2024, doi: 10.1038/s41598-024-52141-0.

- [24] J. Buongiorno, "Convective Transport in Nanofluids," *J Heat Transfer*, vol. 128, no. 3, pp. 240–250, Mar. 2006, doi: 10.1115/1.2150834.
- [25] R. L. Hamilton and O. K. Crosser, "Thermal Conductivity of Heterogeneous Two-Component Systems," *Industrial & Engineering Chemistry Fundamentals*, vol. 1, no. 3, pp. 187–191, Aug. 1962, doi: 10.1021/i160003a005.
- [26] A. Mani and O. Chacko, "Solar radiation climate of India," *Solar Energy*, vol. 14, no. 2, pp. 139–156, Jan. 1973, doi: 10.1016/0038-092X(73)90030-3.
- [27] S. P. P. Sukhatme, J. K. Nayak, and J. K. Naik, *Solar Energy Principles of Thermal Collection and Storage*. 2014.
- [28] J. Facão and A. C. Oliveira, "Experimental uncertainty analysis in solar collectors," *International Journal of Ambient Energy*, vol. 27, no. 2, pp. 59–64, Apr. 2006, doi: 10.1080/01430750.2006.9675004.
- [29] C. Wells and N. R. E. Laboratory, "Measurement techniques applied to PV Performance Uncertainty analysis," 1992. [Online]. Available: <https://docs.nrel.gov/docs/legosti/old/5125.pdf>
- [30] S. A. Mirnezami, N. Huda, R. Saidur, and V. Strezov, "A comprehensive review in pursuit of optimal solar performance: Nanofluids, solar hybrid systems, and challenges ahead," *Sustainable Energy Technologies and Assessments*, vol. 81, p. 104420, Sep. 2025, doi: 10.1016/j.seta.2025.104420.
- [31] F. Khan, M. N. Karimi, and O. Khan, "Exploring the scalability and commercial viability of biosynthesized nanoparticles for cooling panels with the help of Artificial Intelligence and solar energy systems," *Green Technologies and Sustainability*, vol. 1, no. 3, p. 100036, Sep. 2023, doi: 10.1016/j.grets.2023.100036.
- [32] S. H. Majeed *et al.*, "Cooling of a PVT System Using an Underground Heat Exchanger: An Experimental Study," *ACS Omega*, vol. 8, no. 33, pp. 29926–29938, Aug. 2023, doi: 10.1021/acsomega.2c07900.